

Stress and Strain Heuristics for a Layered Elastomeric Foam at Impact Rates

Alexander K. Landauer, Jared Van Blitterswyk, Michael Riley, Aaron M. Forster

Materials Measurement Laboratory

National Institute of Standards and Technology

100 Bureau Drive, Gaithersburg, MD 20899

ABSTRACT

Impact mitigating materials (IMMs) are used to reduce injury or damage due to a blunt impact, which often occurs at high rates or energies. Innovation in IMMs and designs strategies are required for the development of safer protective equipment. A key challenge is translating between idealized experiments (e.g. quasistatic uniaxial stress or high rate Kolsky bar uniaxial strain measurements), fine-grain computational simulations, and real-world performance. To address this challenge, we have coupled high fidelity digital image correlation measurements with drop tower testing, based on our previous work presented to the SEM community. By using digital image correlation, an instrumented drop mass, and an instrumented load plate we obtain spatially and temporally resolved data for a realistic impact scenario. This represents an experimental framework that may be used to guide and validate design criteria applicable to the impact behavior of monolithic and layered IMMs.

Keywords: Impact protection, elastic foam, drop tower testing, digital image correlation, high-speed imaging

INTRODUCTION

Impact mitigating materials (IMMs) are designed and fabricated to minimize the effect of a mechanical insult or hit upon an object to be protected. Typical design targets include, e.g., minimizing linear and rotational accelerations, shock loading, energy transfer, specific or total mass, volume and/or cost, or maximizing energy dissipation [1, 2]. Two design paradigms exist: multi-use and single use. Single use applications can include plasticity or fracture-based solutions, whereas multi-hit applications are constrained to elastic or viscoelastic deformations that are recoverable over the expected time between impacts. Polymer foams, which consist of a crosslinked polymer matrix and gas or fluid filled negative space, are common in both paradigms due to the attractive and tailorable material properties, ease of manufacture and low cost, and adaptability due to the numerous chemistries and foaming processes available [1]. For example, rigid expanded polystyrene foams are ubiquitous for single-impact protection, whereas viscoelastic vinyl-nitrile foams are widely used for multi-impact protection. The uniaxial material response of a typical foam is represented in Fig. 1a, where the large compressive strain domain at relatively constant stress leads to a roughly constant load, i.e., an approximately constant linear acceleration of a protected mass, and the possibility for large energy dissipation if hysteretic mechanisms are active.

Here, we focus on specimens and test techniques for impact mitigation in personal protection, i.e., helmets, pads, or playing surfaces, in which multiple impacts over an $O(1\text{ s})$ time are expected. Typical examples include helmets and padding for contact sports (e.g., football, ice hockey, or lacrosse) and military and police armor and helmets, where impact are $O(10\text{ J})$ and $O(10\text{ ms})$ with strain rates in the padding material reaching 10^1 to 10^2 1/s . In practice, embodiments of protective systems across disciplines often have similar constructions that include a hard shell for penetration or fracture protection and one or more viscoelastic foam (or elastomeric) layers [3]. Foams are often arranged in series to provide both protection and comfort, e.g. a stiff foam adjacent to the exterior shell with an inner soft layer to interface with the head or body during normal use, see the schematic in Fig. 1b. A combination of material and structure are sought that minimize injury risk, either via top-down design, e.g., via models of discrete material layers that minimize stress wave propagation [4, 5] or promote dissipative mechanisms [3] or limit rotational (i.e., shear) loads [6], or via computational topology optimization of lattice-like architected structures [7, 8] which can then be fabricated through additive manufacturing techniques [9]. In this abstract, we discuss a combined instrumented drop tower and digital image correlation (DIC) system to interrogate the response of these structures in real-world impact-like conditions and show an example result for a layered foam.

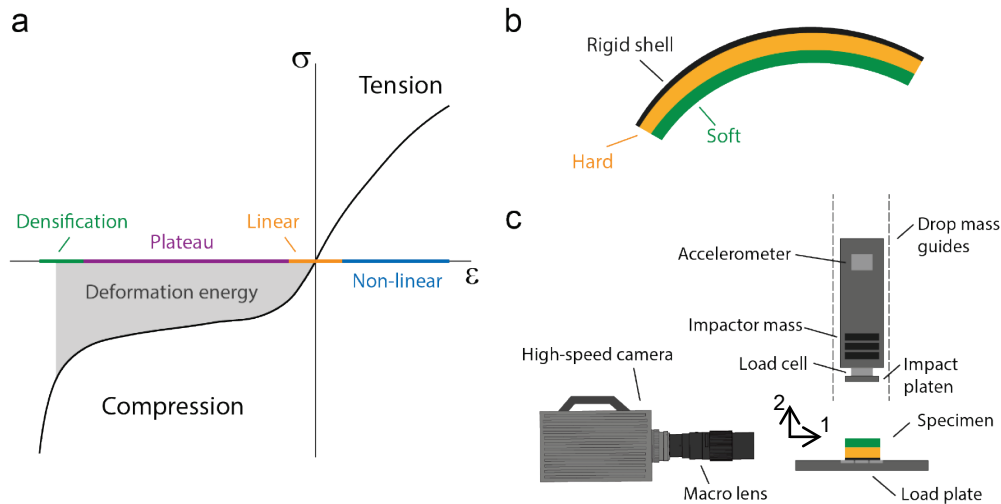


Fig. 1 (a) Typical stress-strain response of a foam-like material at constant strain rate. (b) Simplified schematic of a bi-layer IMM, with hard and soft layers of foam and a rigid external shell. (c) Components (not to scale) of the drop-mass system, including synchronized single camera and load-plate and instrumented (axial load and tri-axial acceleration) adjustable-weight drop mass

METHODS

Foam specimens approximately 50 mm x 50 mm x 25 mm were excised from as-received sheets of a stiff vinyl-nitrile foam (VNW, density approximately 111 kg/m³) and a less stiff vinyl-nitrile foam (VNB, density approximately 135 kg/m³). Both are closed-cell viscoelastic foams. Specimens were either monolithic foam or layered in a VNB (bottom) + VNW (top) or, as in the schematic of Fig. 1b and depicted in Fig. 3a, VNW (bottom) + VNB (top).

For our impact-like (i.e., O(10 J) and O(10 ms)) experiments we employ a custom-designed, instrumented drop-mass, which was previously presented to the SEM community [10]. A custom digital image correlation (DIC) algorithm [11] designed for finite deformations was incorporated into the instrumented drop tower experiments using high-speed imaging, see the schematic in Fig 1c. Typical settings and calibrations for DIC analysis are summarized in Table 1. Images for DIC were captured with a 1:2 macro lens (standoff distance approximately 0.5 m) at a framing rate of 10 kHz (exposure 1/20 000 s, f/5.6). The load plate captured synchronized force data at 50 kHz and the drop mass recorded triaxial accelerations and axial loads on an independent clock. The displacement field data is used to compute the surface strain tensor via a spatial differentiation filter. Strain rate history is computed using temporal central differencing. Table 2 describes the test conditions used in the drop tests. Monolithic materials were subjected to a 0.4 m drop of approximately 12 J of energy. Layered foams were approximately twice the height of the monolithic foams, therefore these were subjected to a 3x increase in energy, approximately 36 J, to achieve a similar degree of compressive strain as the monolithic cases.

RESULTS AND DISCUSSION

The scalar data outputs from the drop mass technique include the peak acceleration of the drop mass, the peak force applied to the top of the specimen, and peak force transmitted through the specimen. These results are given for the monolithic foams and both stack configurations in Table 2. The stiffer VNW was more effective at mitigating a 0.4 m drop (lower peak accelerations and forces) than the softer, but denser, VNB foam. Both foams had relatively short dominant relaxation times -

Table 1 Image and process parameters for digital image correlation of a typical monolithic specimen

Parameter	Value
Camera Noise	0.026%
Prefilter	Gaussian, 3 px by 3 px, $\sigma = 0.5$
Run mode	FFT-based, Hybrid stepping
Image size	818 px by 765 px
Subset size (final)	16 px by 16 px
Step	8 px
Strain filter	Optimal-7 tap
Virtual strain gauge	58 px
Temporal (rate) filter	Central difference
Interpolation	Cubic spline
Measurement points	10185
Total images	235
Static image displacement uncertainty	x: 0.020 px y: 0.019 px
Static image strain uncertainty	$\epsilon_{11} = 427 \mu\text{m/m}$ $\epsilon_{22} = 450 \mu\text{m/m}$ $\epsilon_{11} = 261 \mu\text{m/m}$

Table 2 Drop mass impact data for impacts on monolithic and layered foams. Data are listed as mean \pm one standard deviation for two repeats on two specimens (n = 4) for monolithic foam and two repeats per stack type for layered foam (n = 2)

Specimen	Drop Height (m)	Energy (J)	Peak impactor Acceleration (g)	Peak Applied Force (kN)	Peak Transmitted force (kN)
VNW	0.4	12.3	45.4 \pm 3.5	1.09 \pm 0.11	1.00 \pm 0.07
VNB	0.4	12.3	63.0 \pm 2.6	2.03 \pm 0.07	1.96 \pm 0.06
VNB+	1.2	36.9	81.3 \pm 0.3	2.73 \pm 0.03	2.68 \pm 0.12
VNW+ (top)	1.2	36.9	71.2 \pm 1.9	2.43 \pm 0.06	2.31 \pm 0.06

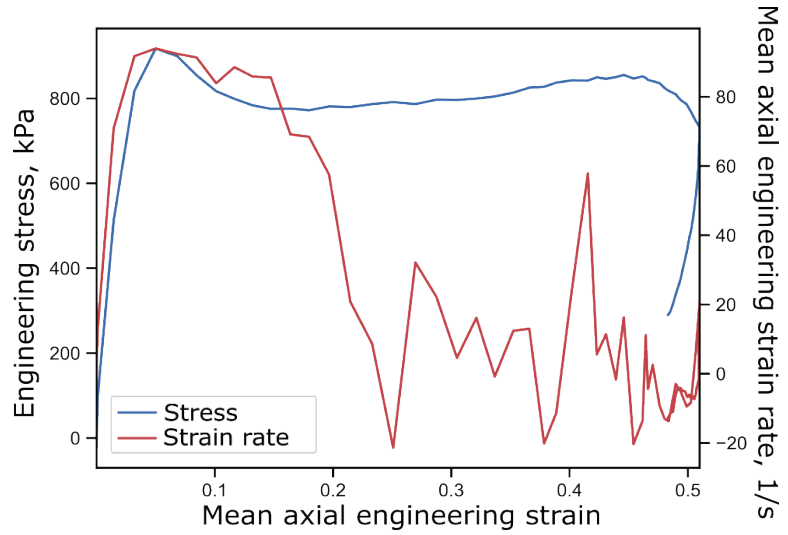


Fig. 2 A typical stress vs. strain and strain-rate vs strain result with mean axial engineering surface strain, ϵ_{22} , and mean axial engineering surface strain rate $\dot{\epsilon}_{22}$ from a 0.4 m impact on VNW

approximately 6.2% and 2.7% residual strain after 100 ms recovery time from impacts of approximately 36.9 J and 12.3 J yielding approximately 83% and 75% axial compressive engineering strain, respectively for VNW and VNB. For the monolithic foam samples, the axial engineering stress (left axis, computed via the measured cross section of the specimen) and the mean full-field axial strain rate (right axis) are plotted as functions of the mean full-field axial engineering strain, see Fig. 2. In this case, the 12.3 J impact leads to approximately 50% strain – enough to initiate an upturn in the stress response (i.e., densification of the foam), although the relative magnitude may be confounded by rate dependency in the material. Note, however, that this is semi-quantitative, since robust boundary conditions (i.e. uniaxial stress) are not established. In the initial loading the strain rate reaches approximately 90 1/s, but as the impact continues this is reduced to less than 20 1/s during the onset of densification.

In the multilayer case, a simple stress versus strain plot holds limited meaning, and instead we use a reduction of the DIC data to interpret the experiment. Peak acceleration and force measurements varied between the VNW+VNB and VNB+VNW configurations, indicating that the stacking order likely leads to measurable differences in impact mitigation. These effects can be further elucidated via the strain history from the DIC analysis. As an example, we take the case of a 36.9 J impact on a VNW+VNB layered foam, the undeformed configuration image of which is shown in Fig. 3a. Since the strain is highly non-uniformly distributed through the height of the specimen, a map of axial strain as a function of height of the specimen (the 2-direction) and post-impact time is given in Fig. 3b. Each time slice represents the mean axial engineering strain ϵ_{22} taken

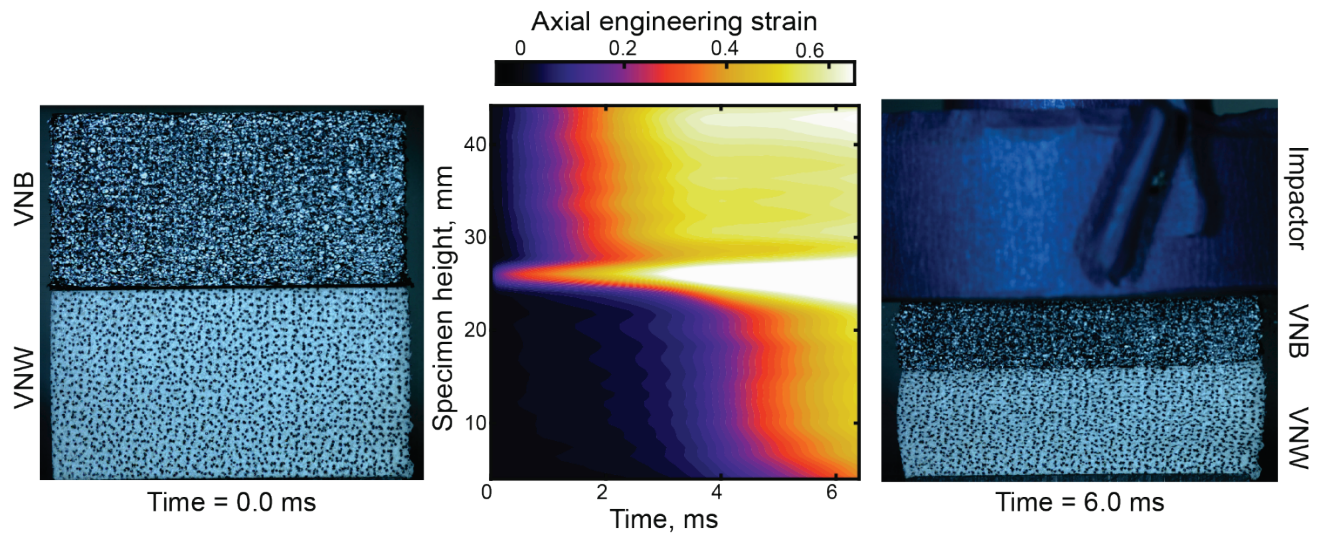


Fig. 3 Snapshot of the multilayer VNW+VNB foam in the undeformed and deformed configurations with the evolution of mean (in the 1-direction) axial strain ϵ_{22} during the first ca. 6 ms of a 36.9 J impact shown as a contour map

across the x_1 direction. From this representation we see that in approximately the initial 2 ms of loading, the top layer deforms relatively uniformly until it reaches saturation at approximately 50% strain (i.e., approaching the densification strain). Apparent strain rapidly builds at the interface – likely an artificial strain since initial conformal contact is not guaranteed at the VNB/VNW interface and speckle pattern characteristic dramatically change – which warrants further investigation since interfaces are typically challenging for accurate DIC measurements. At approximately 4 ms the lower layer begins to rapidly take on strain, although less uniformly than the top layer, and this strain continues to increase beyond 6 ms into the impact event.

CONCLUSION

We have added digital image correlation to the instrumented drop tower experiment and used this to briefly investigate both monolithic and layered foams. The stress-strain and strain rate-strain behaviors, based on full-field measured strains of the specimen surface, are shown during the drop for monolithic foam. An example of layered foam with a strain distribution as a function of time is also given. These measurements highlight the complexity of the impact event compared to the well-controlled conditions of a conventional uniaxial compression test. The extraction of strains from a layered foam system highlights the non-uniformity of the material system response and possibly also the role of interfaces during impact. In the future, 3D-DIC will be employed to establish measurement criteria for elastomeric dissipative materials and the effects of layering strategies will be addressed.

ACKNOWLEDGEMENTS

The authors thank Dwight Barry for assistance fabricating foam specimens.

REFERENCES

- [1] Mills N. *Polymer Foams Handbook: Engineering and Biomechanics Applications and Design Guide*. Elsevier, 2007.
- [2] Gibson LJ, and Michael AF. *Cellular Solids: Structure and Properties*. Cambridge University Press, 1999.
- [3] Duncan O, Shepherd T, Moroney C, Foster L, Venkatraman PD, Winwood K, Allen T, and Alderson A. “Auxetic foams for sports applications.” *Applied Sciences* 8, no. 6 (2018): 941. 10.3390/app8060941.
- [4] Rahimzadeh T, Arruda EM, and Thouless MD. “Design of armor for protection against blast and impact.” *Journal of the Mechanics and Physics of Solids* 85 (2015): 98–111. 10.1016/j.jmps.2015.09.009.

- [5] Sonnenschein MF, Edoardo N, Liangkai M, and Wendt BL. “Impact Mitigation in Layered Polymeric Structures.” *Polymer* 131 (2017): 25–33. 10.1016/j.polymer.2017.10.014.
- [6] Johnston JM, Ning h, Kim JE, Kim YH, Soni B, Reynolds R, Cooper L, Andrews JB, and Vaidya U. “Simulation, fabrication and impact testing of a novel football helmet padding system that decreases rotational acceleration.” *Sports Engineering* 18, no. 1 (2015): 11–20. 10.1007/s12283-014-0160-4.
- [7] Kuhn EN, Miller JH, Feltman B, Powers AK, Sicking D, and Johnston JM. “Youth helmet design in sports with repetitive low- and medium-energy impacts: a systematic review.” *Sports Engineering* 20, no. 1 (2017): 29–40. 10.1007/s12283-016-0215-9.
- [8] Mueller J, and Shea K. “Stepwise graded struts for maximizing energy absorption in lattices.” *Extreme Mechanics Letters* 25 (2018): 7–15. 10.1016/j.eml.2018.10.006.
- [9] Nazir A, Abate KM, Kumar A, and Jeng JY. “A state-of-the-art review on types, design, optimization, and additive manufacturing of cellular structures.” *The International Journal of Advanced Manufacturing Technology* 104, no. 9–12 (2019): 3489–3510. 10.1007/s00170-019-04085-3.
- [10] Forster AM, Riley M. “Metrologies for Performance of Impact Mitigating Materials.” *SEM Annual Conference*, 2017. Indianapolis, IN, USA.
- [11] Landauer AK, Patel M, Henann DL, and Franck C. “A q-Factor-Based Digital Image Correlation Algorithm (qDIC) for Resolving Finite Deformations with Degenerate Speckle Patterns.” *Experimental Mechanics* 58, no. 5 (2018): 815–30. 10.1007/s11340-018-0377-4.